Materials Transactions, Vol. 58, No. 5 (2017) pp. 749 to 756

Evaluation of Ion-Irradiation Hardening of Tungsten Single Crystals by Nanoindentation Technique Considering Material Pile-Up Effect

Eva Hasenhuetl[1,*], Ryuta Kasada[2], Zhexian Zhang[2], Kiyohiro Yabuuchi[2], Yen-Jui Huang[1] and Akihiko Kimura[2]

[1]*Graduate School of Energy Science, Kyoto University, Kyoto 606–8501, Japan*
[2]*Institute of Advanced Energy (IAE), Kyoto University, Uji 611–0011, Japan*

Ion-irradiation hardening of pure tungsten (W) single crystal was evaluated by nanoindentation (NI) technique considering material pile-up effect. Pure W single crystals of (001) surface orientation were ion-irradiated with 6.4 MeV Fe^{3+} to 0.1 dpa, 1 dpa or 2 dpa at 573 K. The irradiation hardening was evaluated by means of NI measurements with elastic-modulus-based correction (EMC) method [C. Heintze *et al.*: J. Nucl. Mater. **472** (2016) 196–205]. The effect of material pile-up in tungsten was so significant that the bulk equivalent hardness values by EMC method were about 70% and 85% of uncorrected results for irradiated and unirradiated W(001), respectively. The ion-irradiation hardening values by EMC based method were approximately 40%, 50% and 60% of uncorrected results for 0.1 dpa, 1 dpa and 2 dpa, respectively. The measured maximum pile-up height was higher for irradiated W(001) than for unirradiated W(001) at each indentation depth. An averaged pile-up height that was associated with the actual area of contact of pile up obtained from EMC hardness showed different responses to ion-irradiation depending on the indentation depth. [doi:10.2320/matertrans.M2016437]

(Received December 8, 2016; Accepted February 22, 2017; Published March 31, 2017)

Keywords: *tungsten, ion-irradiation hardening, hardness, nanoindentation, pile-up*

1. Introduction

Tungsten (W) is a candidate material for plasma facing components in future fusion power plants[1–4]. To simulate fusion environment for W, ion-irradiation is extensively in use[5–10]. A realistic estimation of the actual irradiation hardening behaviour by ion-irradiation experiments in W is essential in order to apply it as a plasma facing component in fusion power reactors. The nanoindentation (NI) technique is a recognized method to measure hardness in ion-irradiated materials, which show a complex distributed damaged layer of a few microns near the irradiated surface. This inhomogeneous defect distribution is a challenge for giving a realistic and representative estimation of expected irradiation hardening behaviour. Analysing the NI-results is not straight forward even for unirradiated materials, since testing artefacts may occur and overlap with phenomena intrinsic to the material. Such testing artefacts can arise from the NI-system itself, for example by the usage of a non-ideal "blunt" indenter shape[11] or by the surface detection technique[12]. Additionally, artefacts may come from insufficient preparation of the testing surface. On the other hand, the indentation size effect (ISE), described by Nix and Gao[13], i.e. increase in hardness with decreasing depth, appears in the obtained NI-profiles, which is considered to be a behaviour that is inevitable for the NI measurement. Furthermore, the softer substrate effect (SSE)[14], can be observed in the NI- profile of a hard thin film on a soft substrate.

The material pile-up or sink-in heights that arise around the permanent indents in the testing material should also be taken into account because of the definition of NI-hardness which depends on the indentation project area of contact as a function of contact depth. The ratio of elastic modulus E_S to yield stress σ, E_S/σ, as well as the hardening coefficient n of the tested material can predict whether pile-up or sink-in will appear in a material[15,16]. Bolshakov and Pharr[16] reported that in materials with a high E_S/σ ratio or alternatively a ratio of final displacement after complete unloading to maximum depth higher than 0.7, $0.7 > h_f/h_{max}$, Oliver and Pharr method[11,15] does not give reasonable results since pile-up is of significant size. This infers that W, having a high E_S/σ ratio, will undergo pile-up while NI-testing.

The pile-up corrected hardness for unirradiated (001) W single crystal has been reported by Lee *et al.*[17,18] who proposed two methods, one by considering a Hertzian loading[19,20] analysis[17] and the other by a determination of the closed contact boundary[18] by an imaging procedure.

Armstrong *et al.*[8] reported that for NI-testing on W–5mass% tantalum alloy (grain with <111>-type surface normal) before and after W ion-irradiation (0.07, 1.2, 13 and 33 dpa at 573 K) the pile-up formation around the indents was affected by the irradiation. They reported that the unirradiated W showed extensive pile-up whereas for damage levels of 0.07 dpa and 1.2 dpa the pile-up was drastically suppressed[8]. However, no corrected hardness method was given in the work. Recently, Heintze *et al.*[21] proposed the so-called elastic-modulus–based correction (EMC) method to correct NI-hardness for pile-up formation. The EMC method[21] uses the square function of indentation modulus to elastic modulus to correct NI hardness. Further, the EMC[21] correction factor involves the reduced elastic modulus which includes the elastic properties of the indenter as well. The EMC method[21] has been evaluated on unirradiated, self-ion irradiated (2.5 dpa and 3.5 dpa at 473 K) and neutron irradiated (2.31 dpa at 473 K) 9% Cr ferritic/martensitic steel T91. Ultrasonic pulse-echo technique results showed no significant difference between the elastic moduli of unirradiated and neutron-irradiated ferritic/martensitic steel T91. Hence, the EMC method[21] is based on the assumption that the elastic modulus is independent of irradiation[21]. Beck *et al.*[22] very recently proposed a method to correct NI-hardness of ion-irradiated (0.24 ±

*Graduate Student, Kyoto University. Corresponding author, E-mail: eva-hasenhuetl@iae.kyoto-u.ac.jp

0.02 dpa at 573 K) W-1mass%Re alloy. They introduced a correction factor C_{cor} that reflected the difference in the actual elastic modulus between the ion-irradiated damaged layer and unirradiated material which were measured by transient grating laser measurements.

We think that the EMC method will be more realistic to consider the effect of the elastic properties of the indenter and the detailed reason will be discussed later. Also, these EMC methods require no thorough measurement of contact areas of remained indenter imprints, although Hardie *et al.*[23] suggested the possible way to measure the actual area of contact by scanning electron microscopy (SEM).

The number of reports about the pile-up effect on NI-hardness of ion-irradiated metals is limited. But in the case of W with a high E_S/σ ratio, the pile-up effect is inevitable and must be considered for evaluating ion-irradiation hardening effects. Because of the above mentioned features and assumptions of the EMC method[21] over the other existing methods, in this study, we evaluated ion-irradiation hardening of W single crystal with consideration of material pile-up effects in order to assess the most feasible analytical method of NI-hardness.

2. Experimental Method

2.1 Material and sample preparation

The material used in this study is a W single crystal with a purity of 99.97%. The surface orientation of the W single crystal has been confirmed to be (001) by electron backscatter diffraction (EBSD) measurement. A detailed description of the material and sample preparation is shown in previous work[7].

2.2 Ion irradiation

Three specimens were irradiated using the dual-beam irradiation experiment test facility (DuET) at Kyoto University[24]. Irradiation with 6.4 MeV Fe^{3+} ions was performed to a nominal displacement damage of 0.1, 1 and 2 dpa, respectively, at 573 K. The target depth profiles of the displacement damage and ion distribution have been calculated using the SRIM (the stopping and range of ions in matter) package[25] and are described in detail in Hasenhuetl *et al.*[7] From SRIM code[25] results, irradiation defects are expected to form up to a penetration depth of approximately 2 μm.

2.3 Nanoindentation tests

NI-tests on the unirradiated and ion-irradiated specimens were carried out using a NanoIndenter G200 of Agilent Technologies Inc., operated with a Berkovich diamond tip. Basic hardness tests, according to Oliver and Pharr's method[11], were carried out at various indentation depths h between 300 nm and 1700 nm at a strain rate target of 0.05 s^{-1}, which is determined by the ratio of loading rate to load, $\dot{P}/P$. The peak load holding time was set to 10 s. Five NI-tests were carried out at each indentation depth h, and one representative test at each indentation depth was considered further. The indenter was positioned such that one side of the Berkovich triangle was perpendicular to a <111> type orientation. NI-tests on each of the specimens were performed in a row to ensure the same azimuthal orientation of the indent with respect to the crystal orientation. The accuracy of the azimuthal indenter orientation has been confirmed by EBSD and can be seen in Fig. 1 for an indent in the unirradiated specimen.

2.4 Pile-up height measurement

In addition to a numerical study, we measured the highest of the three evolved pile-ups around the three sided Berkovich tip by atomic force microscopy (AFM) with scanning in the direction parallel to the <111> orientation

3. Analytical Method for Pile-Up Corrected Hardness:

3.1 Pile-up corrected hardness

According to ISO standards related to NI-testing[26], NI-hardness H_{IT} is the mean contact pressure below the indent and is shown by eq. (1), called the uncorrected NI hardness further on:

$$H_{IT} = F_{max}/A_P{}^{ISO} \tag{1}$$

where F_{max} is the maximum force applied and $A_P{}^{ISO}$ is the projected contact area according to Oliver and Pharr[11]. As for the E-modulus of the NI test system, based on Sneddon's equation[27], Bulychev, Alekhin, Shorokov and their co-workers[28–32] presented the following eq. (2) for a composite modulus E^* (composed of the apparent specimen modulus - the indentation modulus - E_{IT} and indenter modulus, E_I):

$$E^* = \sqrt{\pi} S/(2\beta\sqrt{A_P{}^{ISO}}) \tag{2}$$

where $A_P{}^{ISO}$ is the projected contact area, S is the stiffness considered to be affected by the contact area and a correction factor β for the elastic recovery upon removal of load, which was set to the value of 1.0 in this work.

As it is shown by eq. (2), E^* is inversely proportional to the square root of the projected contact area, which becomes relevant later on in this work. The composite modulus E^* is given by the following equation[11]:

$$1/E^* = (1 - \upsilon s^2)/E_{IT} + (1 - \upsilon_I{}^2)/E_I \tag{3}$$

where E_I is the elastic modulus of the indenter, and υ_I is the corresponding Poisson's ratio. For a diamond Berkovich tip the values are: E_I = 1141 GPa, υ_I = 0.07[11]. E_{IT} is the measured and apparent modulus of the tested material by the G200 testing machine and υ_s is the Poisson's ratio of the tested material (υ_s is 0.28 in the case of W). In Oliver and Pharr's method[11], the stiffness S is obtained by the unloading curve of the indentation from the following equation:

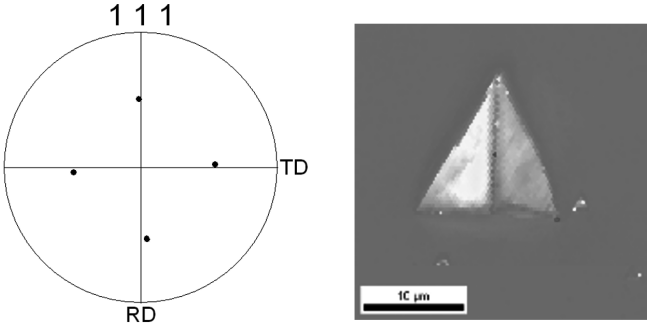

Fig. 1 EBSD pole figure of unirr. W(001) showing the azimuthal orientation of indent with respect to local crystal orientation.

$$h_c^{ISO} = h_{max} - \varepsilon(h_{max} - h_r) = h_{max} - \varepsilon F_{max}/S \quad (4)$$

where $(h_{max} - h_r)$ is the difference between h_{max}, the maximum depth from the initial surface, and h_r, the intercept of the depth axis with the tangent to the unloading curve. $(h_{max} - h_r)$ is further defined by the maximum force applied F_{max} divided by the stiffness S of the tested specimen. ε is a geometric factor, for Berkovich indenters 0.75. The correlation of the different terms of indentation depth are shown in Fig. 2 with $h_{max} = 400$ nm and h_p being the permanent deformation depth in the tested specimen after load removal. Thus, NI hardness H_{IT} and E_{IT} can be obtained from eq. (1) to (4).

From eqs. (1) and (2), a correlation between uncorrected hardness H_{IT} and corrected hardness H^{EMC} can be obtained as shown in eq. (5):

$$H^{EMC} = H_{IT} x A_P^{ISO}/A_P^{EMC} = H_{IT} x (E^{EMC*}/E^*)^2 \quad (5)$$

Based on the findings by Sneddon[27] as well as later on by other researchers, Bulychev, Alekhin, Shorokov and their co-workers[28–32], Heintze *et al.*[21], Beck *et al.*[22] and Hardie *et al.*[23] recently proposed different methods for pile-up corrected hardness. In eq. (5), A_P^{EMC} is the true projected area of contact including pile-up and $E^{EMC}*$ is the calculated composite modulus, in analogy to eq. (3) of the elastic modulus of the indenter E_I and the actual elastic modulus of the material E_S, using $E_I = 1141$ GPa, $\upsilon_I = 0.07$[11] for a diamond tip and $E_S = 410$ GPa[11], $\upsilon_S = 0.28$ for W. Therefore it can be said that E_S is associated with the true projected area of contact including pile-up A_P^{EMC}.

Note that the symbols used in this study as shown in the "List of Symbols" are somewhat different from those in the original works by S. I. Bulychev[28–32], or as in Heintze *et al.*[21], Beck *et al.*[22] and Hardie *et al.*[23] Heintze *et al.*'s[21] pile-up corrected hardness method, which can be called as the elastic modulus correction (EMC) method, was assessed on unirradiated, neutron irradiated and self-ion-irradiated 9 mass% Cr f/m steel T91. An advantage of the EMC[21] method is that one actually does not have to measure the pile-up height, but can use the latter expression of H^{EMC} in eq. (5) that only includes the square of the ratio of $E^{EMC}*$ to E^*. Beck *et al.*[22] also uses the elastic modulus expression, but they don't consider the elastic properties of the indenter in the modulus expressions. Further on, based on their[22] transient grating laser measurement results, they assumed that the elastic modulus of the specimen was changed after ion-irradiation. Hardie *et al.*[23] on the other hand recently used the concept of area expression of eq. (5) to calculate a pile-up corrected hardness for iron ion-irradiated (6.18 dpa at 593 K) Fe-12mass%Cr alloy, $H/A_{actual}/A_{cc}$, which required thorough measurement of the area by scanning electron microscopy (SEM), which is called as the pile-up correction (PUC) method[23].

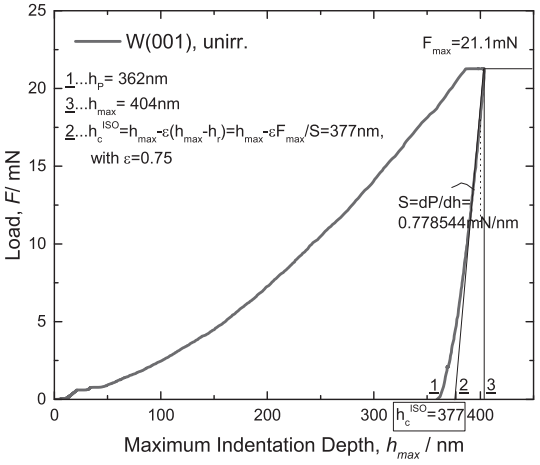

Fig. 2 An example of a F_{max} vs. h_{max} profile for unirr. W(001) up to approximately 400 nm indentation depth.

In the following, we will use the elastic modulus expression of eq. (5) and to some extent the concepts of EMC method by Heintze *et al.*[21] to evaluate the pile-up effect on ion-irradiation hardening in pure (001) W single crystal of various radiation damage levels. What our study has in common with the EMC[21] is that we consider the elastic modulus to be unchanged by irradiation. However, in the case of Heintze *et al.*[22] the elastic modulus (219 GPa) and the measured indentation modulus E_{IT} of unirradiated 9 mass% Cr F/M steel T91 was very stable over indentation depth and similar in magnitude. As will be shown later in Fig. 3 (a), the situation is different in our case, that is in W, firstly because the measured indentation modulus E_{IT} of irradiated as well as unirradiated W(001) varies with indentation depth and secondly the magnitude of both irradiated as well as unirradiated W(001) are about 10% to 35% higher than the target elastic modulus E_S in literature[11], 410 GPa. Therefore, in our study we correct both the unirradiated as well as the irradiated W(001) for pile-up consideration and set the elastic modulus E_S as the target value of the unirradiated W(001), 410 GPa. Also we correct the NI-hardness for each h_{max} individually, which will be shown later. This is contrary to Heintze *et al.*[21], who used an averaged correction factor C_{EMC} for contact depths between 60 nm and 650 nm.

In addition to the EMC method, we were interested in the true projected area of contact including pile-up corresponding to the pile-up corrected hardness H^{EMC}:

$$A_P^{EMC} = F_{max}/H^{EMC} \quad (6)$$

Since describing the full shape of this area, A_P^{EMC}, is difficult, as can be seen in Hardie *et al.*[23], we focused on a so called representative depth including pile-up, $z_{calc.}^{pile\text{-}repr.}$, which is associated with A_P^{EMC} and can be calculated by numerical parameters fit to the Oliver and Pharr method[11].

$$\begin{aligned} A_P^{EMC} = {} & C_0 z_{calc.}^{pile\text{-}repr.2} + C_1 z_{calc.}^{pile\text{-}repr.} \\ & + C_2 z_{calc.}^{pile\text{-}repr.1/2} + C_3 z_{calc.}^{pile\text{-}repr.1/4} \\ & + C_4 z_{calc.}^{pile\text{-}repr.1/8} + C_5 z_{calc.}^{pile\text{-}repr.1/16} \\ & + C_6 z_{calc.}^{pile\text{-}repr.1/32} + C_7 z_{calc.}^{pile\text{-}repr.1/64} \\ & + C_8 z_{calc.}^{pile\text{-}repr.1/128} \end{aligned} \quad (7)$$

The purpose was to gain an understanding of the order of magnitude of an averaged pile-up height $\bar{z}_{calc.}^{pile\text{-}repr.}$:

$$\bar{z}_{calc.}^{pile\text{-}repr.} = z_{calc.}^{pile\text{-}repr.} - h_c^{ISO}. \quad (8)$$

For comparison, we measured the actual highest pile-up height, $\bar{z}_{measured}^{pile\text{-}max.}$, by AFM with scanning in the direction parallel to the <111> orientation.

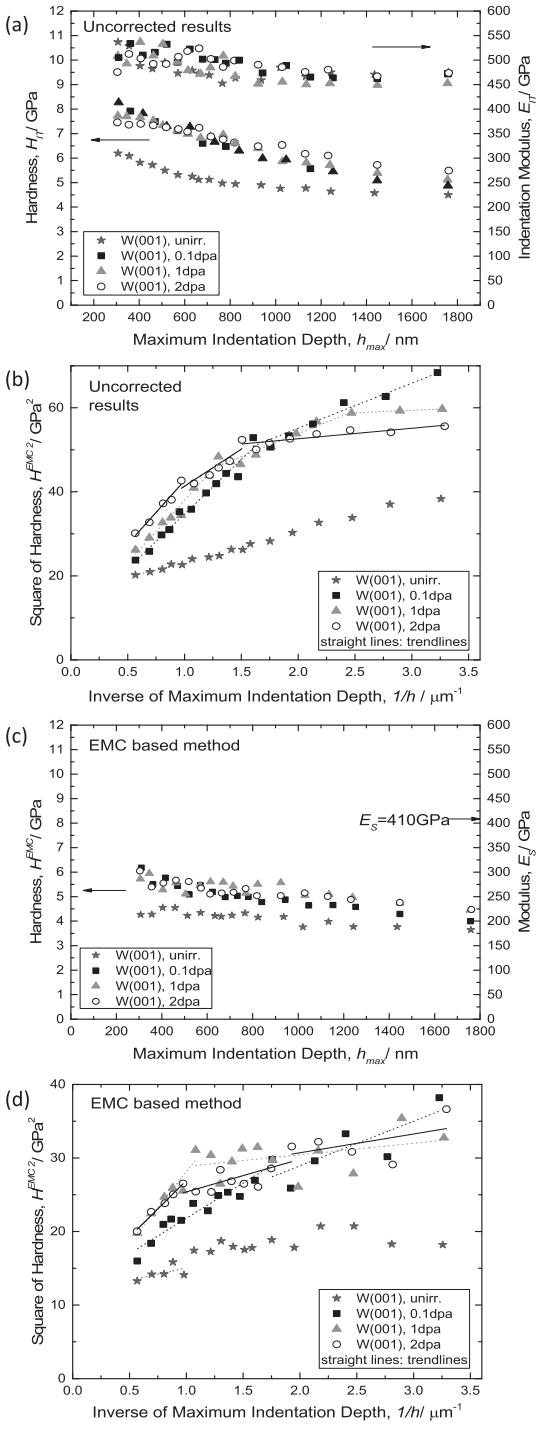

Fig. 3 (a) uncorrected H_{IT} and E_{IT} and (c) corrected H^{EMC} associated with E_S for unirradiated and irradiated W(001). Corresponding Nix-Gao[13] plot for unirradiated and irradiated W(001) of (b) uncorrected and (d) the EMC method[21].

3.2 Ion-irradiation hardening evaluation

The analysis method of ion-irradiation hardening by NI-hardness measurement is based on the Nix-Gao model[13] and Kasada *et al.* method[33]. Nix and Gao developed a model based on the concept of geometrically necessary dislocation[13], which is described in the following equation showing the depth dependence of hardness:

$$H/H_0 = \sqrt{(1 + (h^*/h))} \quad (9)$$

where H is the hardness at a certain indentation depth, h, and H_0 is the hardness at the limit of infinite depth[13]. h^* is a characteristic length that depends on the indenter shape, H_0 and the shear modulus, but is not a constant for a given material and indenter geometry[13]. It is a function of the statistically stored density via H_0[13]. Ideally, plotting the square of the hardness ratio H/H_0 against the reciprocal of the indentation depth shall create a straight line with the slope being h^*, i.e. with a single value of h^* over testing depth[13].

Kasada *et al.*[33] developed NI-techniques on ion-irradiated Fe-based ferritic alloys[33]. They described the depth dependence of hardness by a model that is based on the ISE[13] and extended it by a film/substrate system hardness model based on the Softer Substrate Effect[14] (SSE); the unirradiated region below the irradiated region will be plastically deformed before the indenter itself reaches the unirradiated region. The point of transition is called the critical indentation depth h_{crit} and accounts for the position of the NI-hardness shoulder. With their model[33], the bulk equivalent hardness of the ion irradiated region, $H_{irr}^{bulkequ}$, can be obtained by the least square fitting of the hardness data up to a critical depth h_{crit}. Finally, a single quantitative value to describe irradiation hardening, ΔH, is available as the following equation shows:

$$\Delta H = H_{irr}^{bulkequ} - H_0 \quad (10)$$

4. Results and Discussion

The bulk equivalent hardness, $H_{irr}^{bulkequ}$, which is the hardness at infinite depth H_0 and the resulting irradiation hardening values, ΔH, are given in Table 1. Figure 3 summarizes the results of NI-hardness, indentation modulus as well as the Nix and Gao-plot for evaluation of bulk equivalent hardness[33] and hardness at infinite depth[13] for uncorrected results of the NI-technique and the EMC[21] method. As for the uncorrected results of the NI-technique in Fig. 3(a) and (b), one can see that the indentation modulus E_{IT} varies with h_{max} from approximately 550 GPa in a shallower depth to approximately 450 GPa in a deeper one, which is always above the elastic modulus E_S of W of approximately 410 GPa given by literature[11]. Beck *et al.*[22] also reported a significant increase of indentation modulus in the shallow indentation depth up to

Table 1 Summary of bulk equivalent hardness and irradiation hardening before and after correction by the EMC method[21].

	Uncorrected results				EMC based method[21]			
	unirr.	0.1 dpa	1 dpa	2 dpa	unirr.	0.1 dpa	1 dpa	2 dpa
Bulk equivalent NI-hardness (Nix-Gao) $H_{irr}^{bulkequ.}$ [GPa]	4.05	5.81	7.47	6.90	3.42	4.10	5.22	5.06
ΔH [GPa]		1.76	3.42	2.85		0.68	1.80	1.64

350 nm of about 475 GPa for He^+ implantation (0.24 ± 0.02 dpa at 573 K) in W-1mass%Re alloy and the value was still 420 GPa at 2000 nm h_{max}. In this study, it is considered that this gap between E_{IT} and E_S at each h_{max} is caused by pile-up, which will be taken into account by the EMC[21] method later on in Fig. 3 (c), (d). As mentioned before, it is assumed that the elastic modulus is not changed by irradiation, thus E_s is the target value of E_{IT} for both unirradiated and irradiated W(001). In shallow depths the indentation modulus of unirradiated W(001) is generally lower than irradiated W(001) as can be seen in Fig. 3 (a).

As for the uncorrected NI-hardness, one can see in Fig. 3 (a) that the irradiation effect is still significant at 1700 nm maximum indentation depth and increases with damage level. Hardness shoulder points in the H-h_{max} profile became more pronounced in the Nix and Gao[13] plots in Fig. 3 (b). The plots for 0.1 dpa W(001) showed a hardness-shoulder, whereas interestingly those for 1 dpa and 2 dpa W(001) showed two hardness-shoulders, indicating an appearance at deeper h_{max} at higher damage levels. The SSE[14] seemed to vanish beyond 1000 nm as can be seen in Fig. 3 (b). This led to two stage slopes in the Nix – Gao plot for 0.1 dpa and three stage slopes for 1 and 2 dpa, see Fig. 3 (b). This trend fits well with the microstructural findings in these specimens which will be the focus of another paper.

Figure 3(c), (d) show the H^{EMC} results based on eq. (5) and the Nix – Gao[13] plots for the pile-up corrected hardness method. Comparing Fig. 3(a) with Fig. (c) shows that the NI-profile was roughly shifted by 1 GPa lower as the pile-up corrected hardness method was applied. The hardness-shoulders were slightly shifted and it is unclear from the plots in Fig. 3 (c), (d) whether the 1 dpa W(001) still has two hardness-shoulders after correction or not, since the shallower one might be shifted to a h_{max} that is smaller than the smallest considered h_{max} of about 300 nm after correction. The NI-profiles were not particularly smooth after the correction due to the square function of the correction method. Again, the SSE[14] seemed to vanish beyond 1000 nm as can be seen in Fig. 3 (d). As Table 1 shows, the irradiation hardening of uncorrected results ranges between 1.75 and 3.42 GPa. In both the uncorrected and corrected results by the EMC method, the 1 dpa W(001) exhibits a larger irradiation hardening than the 2 dpa W(001). We believe this fits also with the microstructural findings since the defect density in the shallow depth of a few hundred nm is higher in 1 dpa W(001) compared to 2 dpa W(001), resulting in a larger irradiation hardening. Table 1 indicates that generally, the bulk equivalent hardness values obtained by EMC method were about 70% of the uncorrected results for irradiated W(001) and about 85% for unirradiated W(001), and the irradiation hardening by EMC was approximately 40%, 50% and 60% of uncorrected results for 0.1 dpa, 1 dpa and 2 dpa, respectively. This shows strong influence of pile-up formation on the NI-hardness of ion-irradiated pure (001) W.

The significant pile-up effect on NI-hardness can also be seen when the variation of the term, $H_{IT}/H^{EMC} = {A_P}^{EMC}/{A_P}^{ISO} = (E^*/E^{EMC}*)^2$ is plotted over h_{max} following the eq. (5), see Fig. 4. As a reference, the averaged ratio term, C_{EMC}, of Heintze *et al.*[21] is 1.15 ± 0.05 for neutron irradiated T91 and 1.11 and 1.04 for 2.5 dpa and 3.5 dpa ion-irradiated T91, respectively. Recall that they used a single averaged factor C_{EMC} to correct the hardness over the whole h_{max}. However, in our study they have been calculated individually for every h_{max} and our results show a high dependence of $H_{IT}/H^{EMC} = {A_P}^{EMC}/{A_P}^{ISO} = (E^*/E^{EMC}*)^2$ with h_{max} ranging from 1.45 in shallower h_{max} to 1.15 for deeper h_{max}.

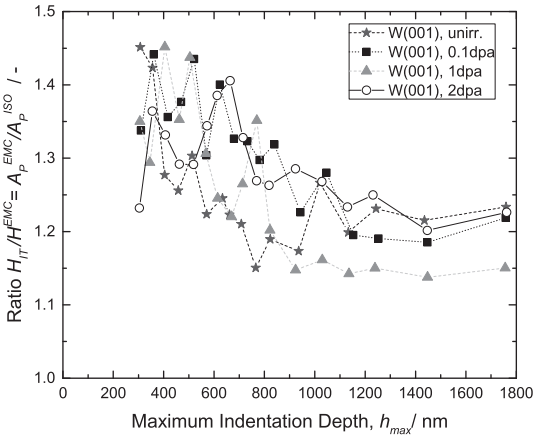

Fig. 4 Variation of the term $H_{IT}/H^{EMC} = {A_P}^{EMC}/{A_P}^{ISO} = (E^*/E^{EMC}*)^2$ over h_{max} for unirradiated and irradiated W(001).

In Fig. 5 (a) and 5 (b), $\bar{z}_{measured.}{}^{pile\text{-}max.}$ and $\bar{z}_{calc.}{}^{pile\text{-}repr.}$ are plotted over h_{max}. The $\bar{z}_{measured}{}^{pile\text{-}max.}$ of unirradiated W(001) shows a linear relationship over h_{max} with a slope of 0.13. In Fig. 5 (a), two results of the measured $\bar{z}_{measured}{}^{pile\text{-}max.}$ per indentation depth are shown to point out the small error bar in the AFM analysis. The evolution of $\bar{z}_{measured}{}^{pile\text{-}max.}$ of irradiated W(001) is more complex than a linear trend. Generally, irradiation caused an increase of $\bar{z}_{measured}{}^{pile\text{-}max.}$ compared to unirradiated W(001) for the same h_{max} and this trend became remarkable with increasing displacement damage. To understand this, one has to look at the 3-dimensional distribution of pile-up around the indents. As we observed in AFM, the volume profile around the indents depended on the irradiation condition. Generally, in the unirradiated specimen, the material pile-up was more broadly distributed and the pile-up height at its maximum was shallower compared to the irradiated specimens. This is in accordance with the work by Hardie *et al.*[23] on Fe-12mass%Cr alloy comparing between as-received and self-ion irradiated condition (6.18 dpa at 593 K) using different indenter shapes. For the results using Berkovich tips, their explanation for the higher pile-up heights in the irradiated Fe-12mass%Cr alloy compared to the unirradiated one was that the plastic zone was suppressed by the ion-irradiated hardened layer, as they showed by TEM observation, and the deformation became more constrained closer to the tip, according to their AFM results. This explanation is reasonable in our case as well.

It should be kept in mind that $\bar{z}_{calc.}{}^{pile\text{-}repr.}$ is an analytical value obtained from ${A_P}^{EMC}$ that serves as a representative pile-up height, but does not reflect the real pile-up height that is in contact with the indenter. However, the $\bar{z}_{calc.}{}^{pile\text{-}repr.}$ values follow an interesting evolution over h_{max}. As mentioned before, $\bar{z}_{measured}{}^{pile\text{-}max.}$ is higher for irradiated W(001) than for unirradiated W(001) at each h_{max}. This is not the case for $\bar{z}_{calc.}{}^{pile\text{-}repr.}$. Although the data is limited, in h_{max} up to 350 nm, irradiated W(001) shows lower $\bar{z}_{calc.}{}^{pile\text{-}repr.}$ than unirradiated

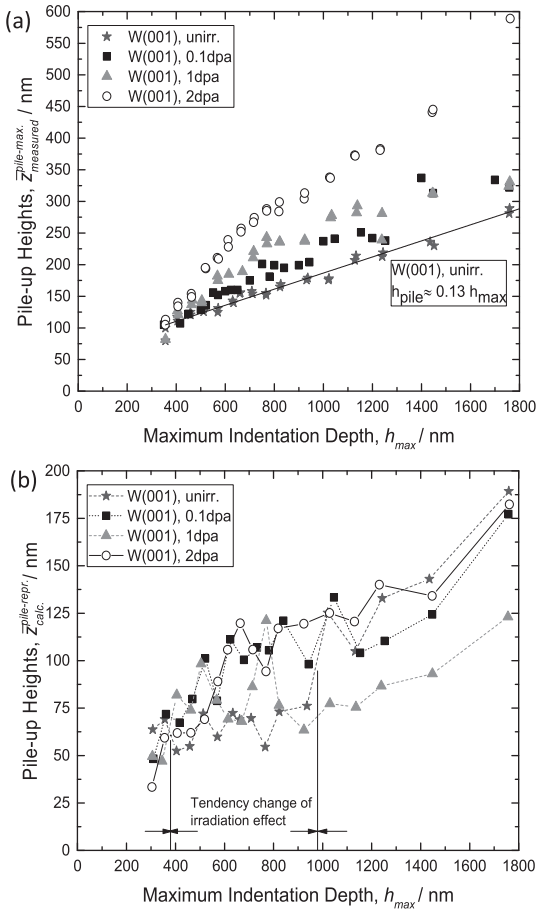

Fig. 5 (a) Calculated $\bar{z}_{calc.}^{pile\text{-}repr.}$ and (b) measured $\bar{z}_{measured}^{pile\text{-}max.}$ over h_{max} for unirradiated and irradiated W(001). Note that the 2 dpa W(001) surface was found to be aligned around 5° to the horizontal plane. So we expect actual pile-up $\bar{z}_{measured}^{pile\text{-}max.}$ to be smaller in this specimen.

W(001). Beyond 350 nm up to 1000 nm, there is a turnover of this trend to an increase of $\bar{z}_{calc.}^{pile\text{-}repr.}$ by irradiation. Beyond 1000 nm, irradiation again reduces $\bar{z}_{calc.}^{pile\text{-}repr.}$ compared to unirradiated W(001). The turnover at 1000 nm h_{max} may be due to the SSE[14] that vanished at this depth according to Fig. 3 (d).

Figure 6 summarizes the ion-irradiation hardening results, based on the eq. (10) of this work in comparison with the previously obtained ion-irradiation results by our group[5] as well as with the neutron-irradiation hardening results by Vickers hardness tests of other researchers[34,35]. The damage levels that are referred to in this figure are averaged damage levels over the projected ion range up to 2000 nm and represent the dpa at a depth of about 600 nm. The bulk-equivalent NI hardness was obtained from the penetration depths from surface to the critical depth showing no softer substrate effect. Therefore we consider that such an averaged dpa value is a good representative for connecting H_0 with dpa.

Zhang *et al.*[5] proposed a method to evaluate bulk equivalent hardness of Fe^{3+} irradiated (2 dpa at 573 K, 773 K, 973 K and 1273 K) pure recrystallized and as received W. The method is based on the assumption that the geometrically necessary dislocation density at an indentation depth is unchanged by ion-irradiation. Their results of ion-irradiation hardening for different irradiation temperatures between 573 K and 973 K are shown in Fig. 6. By converting this temperature

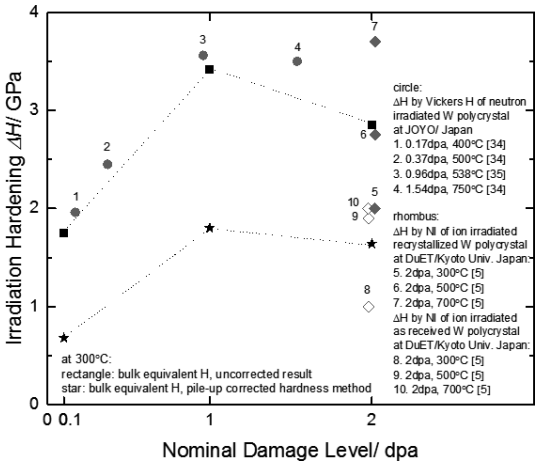

Fig. 6 Summary of ion-irradiation hardening obtained by NI-hardness measurements in this work and comparison with the previous ion-irradiation results by our group[5] as well as with the neutron-irradiation hardening results evaluated by Vickers hardness tests by other groups[34,35].

tendency to our results, it appears that the pile-up corrected ion irradiation hardening results based on the EMC method are consistent with the available neutron-irradiation hardening results[34,35] obtained by Vickers hardness tests for higher temperatures, although the displacement rate effect should be considered.

5. Conclusion

NI-hardness measurements on unirradiated and ion-irradiated (0.1 dpa, 1 and 2 dpa at 573 K) tungsten (W) single crystals of (001) surface orientation were carried out to investigate the ion-irradiation hardening behaviour of pure W with consideration of material pile-up effect using the concepts in the EMC method[21]. The following conclusions can be made:

(1) The magnitude of material pile-up in W is significant. The bulk equivalent hardness values obtained by the EMC method were about 70% of the uncorrected results for irradiated W(001) and about 85% for unirradiated W(001).

(2) The amount of ion-irradiation hardening estimated by the EMC method was approximately 40%, 50% and 60% of uncorrected ones for specimens irradiated up to 0.1 dpa, 1 dpa and 2 dpa, respectively.

(3) The measured maximum pile-up height, $\bar{z}_{measured}^{pile\text{-}max.}$, is higher for irradiated W(001) than for unirradiated W(001) at each h_{max}.

(4) An averaged pile-up height associated with the actual area of contact including pile up from EMC hardness, $\bar{z}_{calc.}^{pile\text{-}repr.}$, showed different responses to ion-irradiation depending on h_{max}. In the case of h_{max} up to 350 nm, irradiated W(001) shows a lower $\bar{z}_{calc.}^{pile\text{-}repr.}$ than unirradiated W(001). Between 350 nm and 1000 nm, there is a turnover of this trend to an increase of $\bar{z}_{calc.}^{pile\text{-}repr.}$ by irradiation. Beyond 1000 nm, irradiation again reduces $\bar{z}_{calc.}^{pile\text{-}repr.}$ compared to unirradiated W(001).

Acknowledgements

Associate Prof. Kondo is thanked for the assistance in operation of Atomic Force Microscope. The financial support of

the first author by the Ministry of Education, Culture, Sports, Science and Technology, MEXT, scholarship of the Japanese Government (1.10.2014 – 30.09.2016) is acknowledged.

Appendix

List of Abbreviations (in alphabetical order)

AFM	Atomic force microscopy.
EBSD	Electron back scatter diffraction.
EMC	Elastic modulus corrected method by Heintze *et al.*[21]
ISE	Indentation size effect[13].
NI	Nanoindentation.
PUC	Pile-up correction method[23].
SEM	Scanning electron microscopy.
SRIM	Stopping range of ions in matter[25].
SSE	Softer substrate effect[14].

List of Symbols (in alphabetical order)

A_P^{EMC}	True projected area of contact including pile-up by EMC method[21].
A_P^{ISO}	Projected contact area according to ISO standards related to NI-testing[26].
β	Factor accounting for the elastic recovery upon removal of load.
C_{cor}	Correction factor by Beck *et al.*[22]
E^*	Composite modulus of elastic modulus of indenter, E_I, and measured modulus of tested material, E_{IT}.
$E^{EMC}*$	Composite modulus of the elastic modulus of the indenter, E_I, and the elastic modulus of the material, E_S.
E_I	Elastic modulus of the indenter.
E_{IT}	Measured and apparent modulus of the tested material.
E_S	Elastic modulus of tested specimen.
F_{max}	Maximum force.
H	NI hardness at a certain indentation depth by Nix and Gao[13].
$H/A_{actual}/A_{cc}$	Pile-up corrected hardness using (PUC) method by Hardie *et al.*[23]
H_0	Hardness at the limit of infinite depth by Nix and Gao[13].
ΔH	Irradiation hardening.
H^{EMC}	Pile-up height corrected NI hardness based on EMC method[21].
H_{IT}	(Uncorrected) NI hardness according to ISO standards related to NI-testing[26].
$H_{irr}^{bulkequ}$	Bulk equivalent hardness of irradiated material by Kasada *et al.*[33]
h^*	Characteristic length[13] that depends on the indenter shape, H_0 and the shear modulus for calculating H_0.
h_c^{ISO}	Contact depth according to ISO standards related to NI-testing[26].
h_f/h_p	Final displacement after complete unloading according to Bolshakov and Pharr[16]/ Permanent deformation depth in the tested specimen after load removal.
h_{max}/h	Maximum indentation depth from the initial surface by ISO standards related to NI-testing[26]/Indentation depth (maximum) by Nix and Gao[13].
h_r	The intercept of the depth axis with the tangent to the unloading curve.
n	Hardening coefficient.
$\dot{P}/P$	Ratio of loading rate to load.
S	Contact stiffness considered to be affected by the contact area.
σ	Yield stress.
υ_I	Poisson's ratio of the indenter.
υ_s	Poisson's ratio of the tested material.
$z_{calc.}^{pile\text{-}repr.}$	Representative depth including pile-up height, associated with A_P^{EMC}.
$\bar{z}_{calc.}^{pile\text{-}repr.}$	Averaged pile-up height, associated with A_P^{EMC}.
$\bar{z}_{measured}^{pile\text{-}max.}$	Measured pile-up height. Highest pile-up located along a <111> orientation.

REFERENCES

1) K. Ezato, S. Suzuki, Y. Seki, K. Mohri, K. Yokoyama, F. Escourbiac, T. Hirai and V. Kuznetcov: Fusion Eng. Des. **98–99** (2015) 1281–1284.
2) M. Merola, F. Escourbiac, A.R. Raffray, P. Chappuis, T. Hirai, S. Gicquel and I.B. Agcy: Fusion Eng. Des. **96–97** (2015) 34–41.
3) H. Bolt, V. Barabash, W. Krauss, J. Linke, R. Neu, S. Suzuki, N. Yoshida and A.U. Team: J. Nucl. Mater. **329–333** (2004) 66–73.
4) A. Hasegawa, M. Fukuda, T. Tanno and S. Nogami: Mater. Trans. **54** (2013) 466–471.
5) Z.X. Zhang, E. Hasenhuetl, K. Yabuuchi and A. Kimura: Nucl. Mater. Eng. **9** (2016) 539–546.
6) Z.X. Zhang, D. Chen, W. Han and A. Kimura: Fusion Eng. Des. **98** (2015) 2103–2107.
7) E. Hasenhuetl, R. Kasada, Z.X. Zhang, K. Yabuuchi and A. Kimura: Mater. Trans. **58** (2017) 580–586.
8) D.E.J. Armstrong, A. Wilkinson and S.G. Roberts: Phys. Scr. **T145** (2011) 014076.
9) D.E.J. Armstrong, P.D. Edmondson and S.G. Roberts: Appl. Phys. Lett. **102** (2013) 251901.
10) J.S.K.L. Gibson, S.G. Roberts and D.E.J. Armstrong: Mater. Sci. Eng. A **625** (2015) 380–384.
11) W.C. Oliver and G.M. Pharr: J. Mater. Res. **7** (1992) 1564–1583.
12) A.C. Fischer-Cripps: Surf. Coat. Tech. **200** (2006) 4153–4165.
13) W.D. Nix and H. Gao: J. Mech. Phys. Solids **46** (1998) 411–425.
14) I. Manika and J. Maniks: J. Phys. D **41** (2008) 074010.
15) W.C. Oliver and G.M. Pharr: J. Mater. Res. **19** (2004) 3–20.
16) A. Bolshakov and G. Pharr: J. Mater. Res. **13** (1998) 1049–1058.
17) Y.-H. Lee, U. Baek, Y.-I. Kim and S.-H. Nahm: Mater. Lett. **61** (2007) 4039–4042.
18) Y. Lee, J. Hahn, S. Nahm, J. Jang and D. Kwon: J. Phys. D **41** (2008) 074027.
19) D. Bahr, D. Kramer and W. Gerberich: Acta Mater. **46** (1998) 3605–3617.
20) W. Gerberich, J. Nelson, E. Lilleodden, P. Anderson and J. Wyrobek: Acta Mater. **44** (1996) 3585–3598.
21) C. Heintze, F. Bergner, S. Akhmadaliev and E. Altstadt: J. Nucl. Mater. **472** (2016) 196–205.
22) C.E. Beck, F. Hofmann, J.K. Eliason, A.A. Maznev, K.A. Nelson and D.E.J. Armstrong: Scr. Mater. **128** (2017) 83–86.
23) C.D. Hardie, S.G. Roberts and A.J. Bushby: J. Nucl. Mater. **462** (2015) 391–401.
24) A. Kohyama, Y. Katoh, M. Ando and K. Jimbo: Fusion Eng. Des. **51–52** (2000) 789–795.
25) "INTERACTION OF IONS WITH MATTER" by J.F. Ziegler. http://www.srim.org/, (accessed 2016-09-17).
26) ISO 14577-1: 2002 Metallic Materials- Instrumented Indentation Test for Hardness and Materials Parameters - Part 1: Test method.

27) I.N. Sneddon: Int. J. Eng. Sci. **3** (1965) 47–57.
28) A. Ternovskii, V.P. Alekhin, M.K. Shorshorov, M. Khrushchev and V. Skvortsov: Zavodskaya Lab. **39** (1973) 1242.
29) S.I. Bulychev, V.P. Alekhin, M.K. Shorshorov, A. Ternovskii and G. Shnyrev: Zavodskaya Lab. **41** (1975) 1137–1140.
30) S.I. Bylychev, V.P. Alekhin, M.K. Shorshorov and A. Ternovskii: Probl. Prochn **9** (1976) 79–83.
31) M.K. Shorshorov, S.I. Bulychev and V.P. Alekhin: Sov. Phys. Dokl. **26** (1982) 769.
32) S.I. Bulychev and V.P. Alekhin: **53** (1987) 1091–1096.
33) R. Kasada, Y. Takayama, K. Yabuuchi and A. Kimura: Fusion Eng. Des. **86** (2011) 2658–2661.
34) T. Tanno, A. Hasegawa, J.C. He, M. Fujiwara, S. Nagomi, M. Satou, T. Shishido and K. Abe: Mater. Trans. **48** (2007) 2399–2402.
35) T. Tanno, M. Fukuda, S. Nogami and A. Hasegawa: Mater. Trans. **52** (2011) 1447–1451.